# EXPERIMENTAL STUDY OF LATERALLY OFFSET RHS X-CONNECTIONS

FEI WEI[1] and JEFFREY A. PACKER[1*]

[1]*Department of Civil & Mineral Engineering, University of Toronto, Ontario M5S 1A4, Canada E-mail: jeffrey.packer@utoronto.ca*

Aside from the most common approach to designing and fabricating welded Rectangular Hollow Section (RHS) connections, occasions may occur when it is desired to have branch (web) members laterally offset from the centerline of the chord member. However, the design rules included in all contemporary codes and design guides merely apply to connections without offset in the transverse direction. Thus, to investigate the effect of laterally offset members on the strength of these connections, a laboratory-based experimental program consisting of 12 full-scale connection tests has been conducted on cold-formed RHS-to-RHS X-connections with the branch loaded in quasi-static axial compression. Comparison has been made between the structural behavior of laterally offset connections and their standard counterparts, where appropriate. Recommendations are made for handling such laterally offset RHS X-connections on the basis of current design standards, and an analytical model is proposed and evaluated to give a good prediction of the static strength.

*Keywords*: Rectangular hollow sections, connections, joints, branch offset, experimentation.

## 1 Introduction

Extensive research has been conducted over the past decades to investigate the static behavior of truss-type, welded rectangular hollow structural section (RHS) connections. The results have led to a number of prominent codes and design guides, such as CIDECT DG3 (Packer et al. 2009), AISC 360-16 (AISC 2016), EN 1993-1-8 (CEN 2005) and ISO 14346 (ISO 2013). These hollow section design recommendations presume that, for RHS connections, the branch (web) centerlines intersect with the chord centerline. Sometimes it is desirable to have branch members laterally offset from the central plane of the chord and, in practice, these laterally offset connections may allow economical and easy installation of cladding materials, as shown in Fig. 1.

Figure 1. Application of laterally offset RHS connections

*Proceedings of the 17th International Symposium on Tubular Structures.*
*Editors:* X.D. Qian and Y.S. Choo

*Published by* Research Publishing, Singapore.
ISBN: 978-981-11-0745-0; doi:10.3850/978-981-11-0745-0_049-cd

However, it is uncertain how such an offset may influence the structural behavior of RHS connections, and the design rules included in all contemporary codes merely apply to connections without offset in the transverse direction. With the existence of laterally offset connections in practice, and the lack of design guidelines for such, it is worth to investigate the static behavior of laterally offset connections and to make comparisons against their standard counterparts.

This paper specifically investigates the structural behavior of laterally offset RHS X-connections. A series of 12 full-scale connection tests, consisting of eight laterally offset and four non-offset configurations, is thus conducted on cold-formed RHS X-connections with the branch members loaded in axial compression. The four non-offset cases, together with some previous laboratory experiments on standard RHS X-connections (Fan and Packer 2017), are used as control specimens for comparison with the laterally offset specimens.

## 2 Analytical Models

The design approaches and the equations used to predict the strength of standard welded RHS X-connections, without the branch offset, are well studied.

### 2.1 *Chord face plastification*

When a connection has a branch-to-chord width ratio of $\beta \leq 0.85$ without any offset (defined as a "stepped" connection), the failure mode is usually governed by the limit state of chord face plastification. The yield load $N_1$, associated with chord face plastification, can be derived based on a flexural rectilinear yield line mechanism formed in the chord face, as shown in Fig. 2.

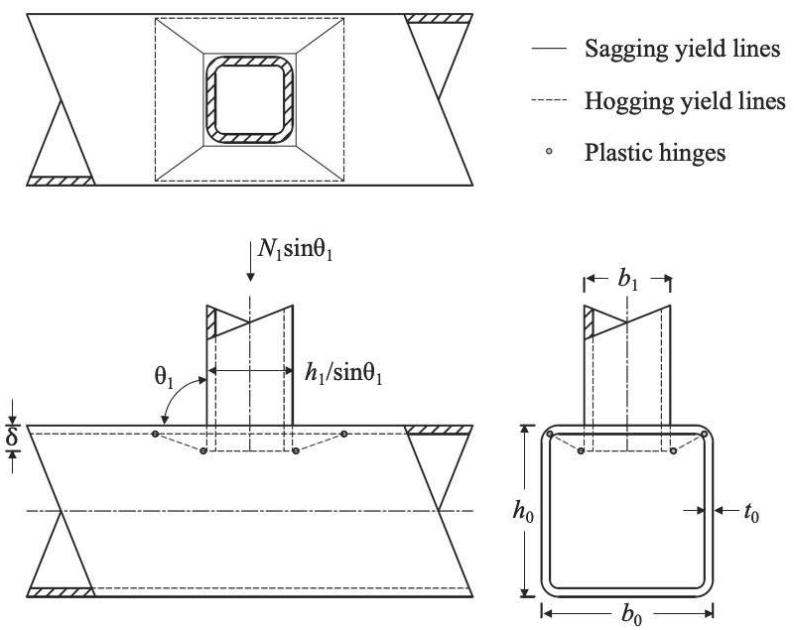


Figure 2. Yield line mechanism for a stepped RHS-to-RHS axially loaded X-connection

This approach has been widely adopted in various design recommendations for RHS-to-RHS X-, T-, and Y-connections. With a chord yield stress of $f_{y0}$, the yield load is given as:

$$N_1 \sin\theta_1 = \frac{f_{y0} {t_0}^2}{(1-\beta)} \left( \frac{2\eta}{\sin\theta_1} + 4\sqrt{1-\beta} \right) Q_f \qquad (1)$$

where η is the ratio of branch depth to the chord width ($h_1/b_0$), and $Q_f$ is a reduction factor to account for the effect of normal stress in the chord. The validity limit of this limit state is capped at β = 0.85, since the predicted load will lead to infinity as β approaches unity.

### 2.2 *Chord sidewall failure in compression*

Once β reaches unity, the connection becomes a full-width matched connection, where the branches have the same width as the chord. Thus, the branch loads are primarily resisted by two chord sidewalls. For such connections, the capacity is governed by chord sidewall failure instead of chord face plastification.

A recent numerical study of welded, full-width, RHS-to-RHS X-connections with the branches in axial compression by Kuhn et al. (2019) supported the practice of CIDECT (Packer et al. 2009) and ISO 14346 (ISO 2013) whereby each chord sidewall is treated as a column. The combined sidewall compression strength, by this method, is given by the general expression:

$$N_1 \sin\theta_1 = 2\chi f_{y0} t_0 \left(\frac{h_1}{\sin\theta_1} + 5t_0\right) Q_f \tag{2}$$

where χ is a reduction factor applied to yield stress for column buckling and should be calculated based on a slenderness ratio of $KL/r$. The radius of gyration, $r$, of a rectangular cross section HSS wall is $t/\sqrt{12}$. The effective length factor, $K$, can be determined according to the end fixity, applied to a column length, $L$, of the sidewall flat dimension. The end fixity of the sidewall "column" is close to fixed-fixed for fully welded X-connections and, for these end conditions, $K$ can be taken as 0.65. Kuhn et al. (2019) noticed that most steel codes have a cold-formed column buckling curve which is almost linear when plotted over a practical chord sidewall slenderness range. Thus, Kuhn et al. (2019) advocated a simple and conservative estimation for χ using Eq. (3), for fixed-fixed end conditions, which gave an excellent fit to numerical data:

$$\chi = 1.15 - 0.013\frac{h_1}{t_0}\sqrt{\frac{1}{\sin\theta_1}} \leq 1 \tag{3}$$

Furthermore, Kuhn et al. (2019) showed that χ should be taken as 1.0 (implying a chord sidewall local yielding failure mode) when the bearing length ($h_1/\sin\theta_1$) ≤ $0.25h_0$. Eq. (3) is subject to limits of validity of $f_y \leq 350$ MPa and $h_0/t_0 \leq 50$.

### 2.3 *Combined chord failure*

When the branch of a stepped connection is moved towards the chord sidewall, as shown in Fig. 1, a laterally offset connection is formed. For such connections, the failure may involve chord face plastification together with the failure of the particular chord sidewall that the branch is bearing against. To account for this failure mode, a combined yield line mechanism is proposed to predict the strength of a laterally offset RHS-to-RHS X-connection, as shown in Fig. 3. By virtual work, the derived failure load is:

$$N_1 \sin\theta_1 = 2f_{y0}{t_0}^2 \left[\frac{\eta}{4(1-\beta)} + \gamma\eta\chi + \sqrt{\frac{1}{1-\beta} + 2\gamma\chi}\right] Q_f \tag{4}$$

where γ is the chord slenderness ratio of $b_0/2t_0$, and χ can be calculated using the appropriate $K$ factor for the sidewalls. A validity limit of $(1 - \beta) \geq 0.075$, or $\beta \leq 0.925$, would be appropriate. This failure mechanism is evaluated against the laboratory tests later in this paper.

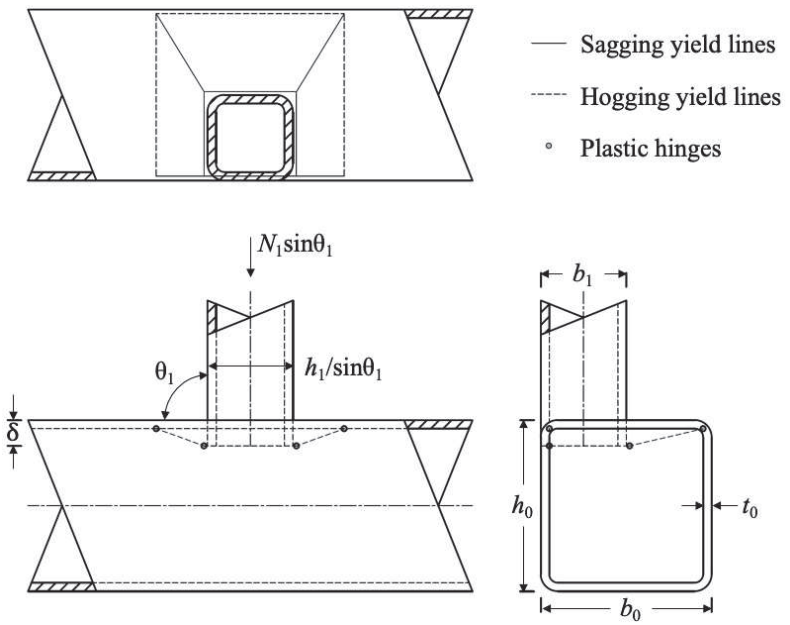


Figure 3. Combined yield line mechanism for a laterally offset RHS-to-RHS axially loaded X-connection

## 3 Experimentation

The experimental program included material property tests and 12 full-scale welded RHS-to-RHS 90° X-connection tests, with eight having branch(es) fully offset to the chord sidewall (X1 to X4 and T1 to T4) and four having non-offset branches (X5, X6, T5 and T6), as listed in Table 1.

**Table 1.** Test specimens and measured dimensions

| Specimen | $b_0\times h_0\times t_0$ (mm) | $b_1\times h_1\times t_1$ (mm) | Width ratio (β) | Chord slenderness ratio (2γ) | Chord length (mm) | Branch length (mm) | Weld size* (mm) |
|---|---|---|---|---|---|---|---|
| X1 | 202.7×202.7×5.8 | 101.2×101.2×12.4 | 0.50 | 34.9 | 1107 | 505 | 5.2 |
| X2 | 204.0×204.0×8.6 | 101.2×101.2×12.4 | 0.50 | 23.7 | 1102 | 503 | 5.0 |
| X3 | 202.7×202.7×5.8 | 152.4×152.4×11.6 | 0.75 | 34.9 | 1162 | 508 | 5.8 |
| X4 | 204.0×204.0×8.6 | 152.4×152.4×11.6 | 0.75 | 23.7 | 1158 | 502 | 5.4 |
| X5 | 202.7×202.7×5.8 | 203.7×102.1×12.7 | 1.00 | 34.9 | 1053 | 506 | 6.4 |
| X6 | 204.0×204.0×8.6 | 203.7×102.1×12.7 | 1.00 | 23.7 | 1007 | 505 | 5.5 |
| T1 | 202.7×202.7×5.8 | 101.2×101.2×12.4 | 0.50 | 34.9 | 1068 | 505 | 6.4 |
| T2 | 204.0×204.0×8.6 | 101.2×101.2×12.4 | 0.50 | 23.7 | 1028 | 504 | 7.4 |
| T3 | 202.7×202.7×5.8 | 152.4×152.4×11.6 | 0.75 | 34.9 | 1164 | 506 | 4.4 |
| T4 | 204.0×204.0×8.6 | 152.4×152.4×11.6 | 0.75 | 23.7 | 1162 | 501 | 5.6 |
| T5 | 202.7×202.7×5.8 | 203.7×102.1×12.7 | 1.00 | 34.9 | 1024 | 502 | 7.3 |
| T6 | 204.0×204.0×8.6 | 203.7×102.1×12.7 | 1.00 | 23.7 | 1002 | 500 | 7.0 |

*leg size of fillet welds

### 3.1 *Geometric and material properties*

All members were made of cold-formed RHS to either ASTM A500 (ASTM 2018) or CSA G40.20/G40.21 (CSA 2013), and two designated chord sizes were used: HSS 203×203×6.4 and HSS 203×203×9.5. Three designated branch sizes were selected: HSS 102×102×12.7, HSS 152×152×12.7 and HSS 203×102×12.7. This enabled three nominal β value of 0.5, 0.75 and 1.0, with two nominal 2γ values of 21.4 and 31.7. The detailed specimen configurations with measured dimensions are tabulated in Table 1.

The branch thickness was selected to be greater than that of the chord, to be certain that local branch yielding would not occur before chord sidewall failure. Mechanical properties of the two chord members were determined by tensile tests on coupons cut from the flat regions where there was no weld seam. Average measured values (using three coupons from each chord) for modulus of elasticity ($E$), yield stress ($f_y$), yield strain ($\varepsilon_y$), ultimate stress ($f_u$) and rupture strain ($\varepsilon_{rup}$), are presented in Table 2.

**Table 2.** Average measured mechanical properties

| Designation (mm) | $E$ (MPa) | $f_y$ (MPa) | $\varepsilon_y$ | $f_u$ (MPa) | $f_y/f_u$ | $\varepsilon_{rup}$ |
|---|---|---|---|---|---|---|
| HSS 203×203×6.4 Chord | 208100 | 393.6 | 0.0039 | 484.4 | 0.81 | 0.308 |
| HSS 203×203×9.5 Chord | 197400 | 392.5 | 0.0040 | 494.0 | 0.79 | 0.334 |

### 3.2 *Laboratory testing set-up*

All 12 connections were fabricated and tested to failure under displacement control, in quasi-static branch compression, using a 5000 kN-capacity Baldwin universal testing machine. As in the example of Fig. 4(a), for specimens X1 to X6 branches were welded on both sides of the chord. The branch compression load was reacted by a steel plate, which was secured to the laboratory strong floor. To prevent any possible lateral movements caused by global buckling of the specimen, two threaded rods were used to laterally restrain the test specimen by bracing to the testing machine frame. Such lateral restraint of the connection was considered to be comparable to what would be generally provided to an offset connection by the surrounding structure.

(a) Offset branches welded on both sides (X2) (b) Full-width branch welded on only one side (T5)

Figure 4. Typical testing setups

To compare with previous tests conducted by Fan and Packer (2017) on stepped connections, specimens T1 to T6 were fabricated with only one branch, hence T-shaped connections were

supported and secured to a steel frame instead, as shown in Fig. 4(b). These T-shaped specimens are still technically X-connections because transverse load is transmitted through the chord member. Testing T-shaped specimens in this manner was useful for Fan and Packer (2017) to investigate chord face failure (with $\beta \leq 0.85$), without the complication of evaluating the effect of chord bending moments (Packer et al. 2017).

The displacement for each laboratory test was captured at many points by a Metris K-610 3D Dynamic Laser Measuring System together with a Linear Variable Differential Transformer (LVDT).

## 4 Evaluation of Results

All 12 connection tests failed by global buckling of one or both chord sidewalls, depending on whether the branch was offset or not, and the peak load ($N_{1,max}$) was achieved prior to the $3\%b_0$ connection ultimate deformation limit state (Lu et al. 1994). Thus, the connection ultimate strength was given by $N_{1,exp} = N_{1,max}$, and the test results are summarized in Table 3.

**Table 3.** Test results

| Specimen | Experiment $N_{1,exp}$ (kN) | Analytical Model* $N_{1,model}$ (kN) | $\frac{N_{1,exp}}{N_{1,model}}$ | Specimen | Experiment $N_{1,max}$ (kN) | Analytical Model* $N_{1,model}$ (kN) | $\frac{N_{1,exp}}{N_{1,model}}$ |
|---|---|---|---|---|---|---|---|
| X1 | 313 | 268 | 1.17 | T1 | 340 | 226 | 1.50 |
| X2 | 564 | 561 | 1.01 | T2 | 607 | 513 | 1.18 |
| X3 | 416 | 355 | 1.17 | T3 | 412 | 299 | 1.38 |
| X4 | 722 | 741 | 0.97 | T4 | 735 | 679 | 1.08 |
| X5 | 569 | 349 | 1.63 | T5 | 595 | 274 | 2.17 |
| X6 | 1084 | 793 | 1.37 | T6 | 1083 | 701 | 1.55 |

* Offset specimens X1 to X4 and T1 to T4 are predicted by Eq. (4); full-width specimens X5, X6, T5 and T6 are predicted by Eq. (2). The sidewall flat dimension is taken as $(h_0 - 3t_0)$, per AISC 360 (AISC 2016). $K = 0.65$ is used for X-shaped connections; $K = 0.80$ is used for T-shaped connections.

### 4.1 *Comparison with analytical models*

The connection strengths predicted using the proposed models are also included in Table 3, given as $N_{1,model}$, to compare with the experimentally determined strength ($N_{1,exp}$). The strength of laterally offset connections (specimens X1 to X4 and T1 to T4) was predicted using Eq. (4). For the remaining four full-width connections, the strength was predicted by Eq. (2). Since the Eq. (3) simplification is only applicable to X-connections with two welded branches, for consistency the reduction factor ($\chi$) was calculated throughout by using $K = 0.65$ (for X-shaped connections) or $K = 0.80$ (for T-shaped connections), in conjunction with the column buckling curve of AISC 360 Chapter E (AISC 2016). For the T-shaped connections with one welded branch the end fixity of the sidewall "column" is close to fixed-pinned rather than fixed-fixed. The measured geometric and material properties were used in all strength predictions with the weld sizes not taken into account, since designers do not know the exact size of the weld until the connections have been detailed and fabricated.

For the eight laterally offset connections, the actual/predicted strength has a mean of 1.20 and an associated coefficient of variation (COV) of 0.16. This shows that the proposed analytical model (Fig. 3) is a good predictor of the laterally offset connections and can be safely used for design purposes.

### 4.2 *Comparison with standard connections*

The load-displacement curves of three typical T-shaped connection tests are presented in Fig. 5, with the connection strength and the deformation limit marked. Connection displacement was determined from the global vertical displacement between light-emitting-diode (LED) targets placed on the branch slightly above the chord face and the fixed pedestal (reaction). The branch compression load was provided by the testing machine's load cell.

With a chord member of the same nominal dimension (HSS 203×203×6.4), the three connection tests included in Fig. 5 are: a laterally offset connection (T1) with $\beta = 0.5$, a non-offset stepped connection with the same-size branch and $\beta = 0.5$, and a full-width matched connection ($\beta = 1.0$) with the same bearing length (T5). The detailed geometric and material properties of the stepped connection can be obtained from specimen X-0.5-32-700O by Fan and Packer (2017), where the laboratory test was conducted in a very similar manner.

As can be seen from Fig. 5, with a same-size branch, the static strength of a laterally offset connection is about two to three times as much as that of a non-offset stepped connection. Nevertheless, with the same bearing length, the strength is significantly lower than that of the full-width matched connection. A similar trend is also observed through a comparison between the strength of specimen T2 (607 kN), X-0.5-21-550O (311 kN) by Fan and Packer (2017) and T6 (1083 kN), with approximately the same chord member of HSS 203×203×9.5. Thus, it would be excessively conservative to design a laterally offset connection in a similar manner to the non-offset stepped connection using Eq. (1), which is included in most prominent codes and design guides.

As discussed earlier, for laterally offset connections, failure involves the buckling of one sidewall together with chord face plastification to a certain extent. Therefore, the strength of such connections can be quickly and conservatively estimated by taking a 50% reduction in capacity of the full-width connection with the same bearing length, and this is supported by the results of the test program. By comparing the strength of full-width connections (X5, X6, T5 and T6) against the strength of laterally offset connections with the same bearing length (X1, X2, T1 and T2), the offset-to-full width connection strength ratio averages 0.55.

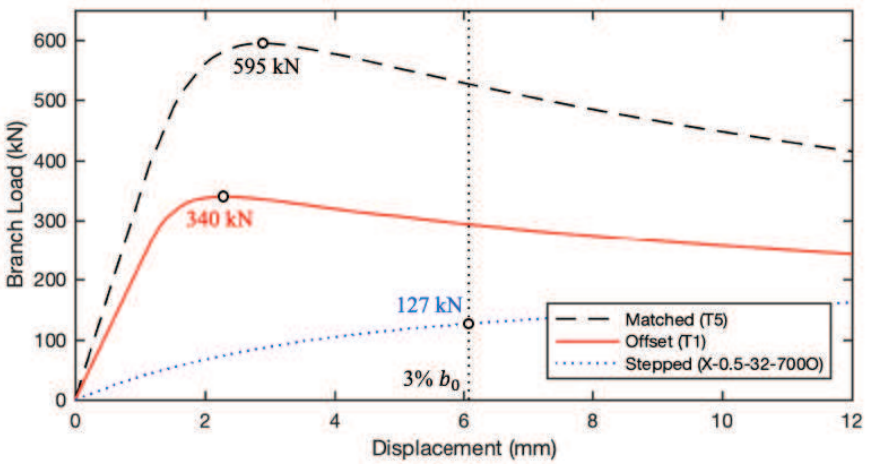


Figure 5. Typical load-displacement curves for HSS 203×203×6.4 chord, with offset and stepped connections having $\beta = 0.5$ and all connections having the same bearing length

## 5 Conclusions and Recommendations

From 12 full-scale welded RHS-to-RHS 90° X-connection tests in branch compression, together with previous laboratory experiments conducted by Fan and Packer (2017), it has been found that, in the case of connections with branches fully offset to the chord sidewall, the static strength is about twice as much as that of their counterparts with the same-size branch members without any offset; however, the strength is about 50% lower than that of the full-width connection with the same bearing length. Hence, it is recommended that, when the branch of a connection is fully offset to the chord sidewall, the capacity can be estimated by reducing the strength predicted by Eq. (2) by 50%. Alternatively, the failure load predicted by a combined yield line mechanism (Fig. 3) is shown to correspond well with the laboratory test results and can thus be well-estimated by Eq. (4). The conclusions apply to laterally offset RHS-to-RHS axially-loaded T-, Y- and X-connections with $\beta \leq 0.925$.

## Acknowledgments

Financial support for this project was provided by the Natural Sciences and Engineering Research Council of Canada (NSERC). Hollow structural sections used for experiments reported herein were donated by Atlas Tube, Harrow, Ontario.

## References

AISC, *ANSI/AISC 360-16, Specification for Structural Steel Buildings,* American Institute of Steel Construction, Chicago, 2016.

ASTM, ASTM A500/A500M-18, Standard Specification for Cold-Formed Welded and Seamless Carbon Steel Structural Tubing in Rounds and Shapes, American Society for Testing and Materials, West Conshohocken, 2018.

CEN, EN 1993-1-8, Eurocode 3: Design of Steel Structures - Part 1-8: Design of Joints, European Committee for Standardization, Brussels, 2005.

CSA, CSA G40.20-13/G40.21-13, General Requirements for Rolled or Welded Structural Quality Steel, Canadian Standards Association, Toronto, 2013.

Fan, Y. and Packer, J. A., RHS-to-RHS Axially Loaded X-Connections Near an Open Chord End, *Can. J. Civ. Eng*. 44, 881-892, 2017.

ISO, ISO 14346, Static Design Procedure for Welded Hollow Section Joints – Recommendations, International Organization for Standardization, Geneva, 2013.

Kuhn, J., Packer, J.A. and Fan, Y., RHS Webs under Transverse Compression, *Can. J. Civ. Eng.* 46, 2019.

Packer, J.A., Puthli, R., van der Vegte, G.J. and Wardenier, J., Discussion on "Experimental and Numerical Assessment of RHS T-Joints subjected to Brace and Chord Axial Forces" by Nizer et al., *Steel Construction – Design and Research* 10, 89-90, 2017.

Packer, J.A., Wardenier, J., Zhao, X.-L., van der Vegte, G.J. and Kurobane, Y., CIDECT Design Guide No.3, Design Guide for Rectangular Hollow Section (RHS) Joints under Predominantly Static Loading, 2nd Ed., CIDECT, Geneva, 2009.